

Submitted to the Specialists Meeting on Shielding Aspects of Accelerators, Targets and Irradiation Facilities, Knoxville, USA, September 17-18, 1998.

RECEIVED  
SEP 28 1999  
OSTI

## Further Measurements of Bremsstrahlung from the Insertion Device Beamlines of the Advanced Photon Source

P. K. Job, M. Pisharody and E. Semones, Experimental Facilities Division, Argonne National Laboratories, 9700 S. Cass Ave., Argonne IL 60439, USA

### Abstract

Bremsstrahlung is produced in the Advanced Photon Source (APS) storage ring when the positron beam interacts with the storage-ring components or with the residual gas molecules in the storage-ring vacuum. The interaction of the positrons with the gas molecules occurs continually during storage-ring operation. Bremsstrahlung is important at the insertion device straight sections because the contribution from each interaction adds up to produce a narrow mono-directional beam that travel down the beamlines. At the APS, with long storage ring beam straight paths (15.38 meters), gas bremsstrahlung in the insertion device beamlines can be significant. The preliminary results of the bremsstrahlung measurements in the insertion device beamlines of the APS was presented at SATIF3. This paper presents the results of further measurements at the two insertion device(ID) beamlines with higher statistics in the data collection. The beam current and the vacuum normalized bremsstrahlung power is fairly constant in a beamline for a given storage ring fill pattern, but may vary from beamline to beamline. The average bremsstrahlung power is measured as  $118 \pm 9$  GeV/s/nT/mA at beamline 11 ID and as  $36 \pm 2$  GeV/s/nT/mA at beamline 6 ID. These results, along with the results from the four previous independent bremsstrahlung measurements, enabled us to conclude upon the various reasons causing this variation.

The submitted manuscript has been authored by a contractor of the U.S. Government under contract No. W-31-109-ENG-38. Accordingly, the U.S. Government retains a nonexclusive, royalty-free license to publish or reproduce the published form of this contribution, or allow others to do so, for U.S. Government purposes.

---

Work supported in part by US Department of Energy, Contract No. W-31-109-ENG-38, BES-Material Science, Argonne National Laboratory.

## **DISCLAIMER**

This report was prepared as an account of work sponsored by an agency of the United States Government. Neither the United States Government nor any agency thereof, nor any of their employees, make any warranty, express or implied, or assumes any legal liability or responsibility for the accuracy, completeness, or usefulness of any information, apparatus, product, or process disclosed, or represents that its use would not infringe privately owned rights. Reference herein to any specific commercial product, process, or service by trade name, trademark, manufacturer, or otherwise does not necessarily constitute or imply its endorsement, recommendation, or favoring by the United States Government or any agency thereof. The views and opinions of authors expressed herein do not necessarily state or reflect those of the United States Government or any agency thereof.

## **DISCLAIMER**

**Portions of this document may be illegible  
in electronic image products. Images are  
produced from the best available original  
document.**

## Introduction

High-energy electron storage rings generate energetic bremsstrahlung photons through radiative interaction of the electrons (positrons) with the storage-ring components or with the residual gas molecules inside the vacuum chamber. The resulting radiation exits at an average emittance angle of  $mc^2/E$  radian with respect to the electron beam path, where  $mc^2$  is the rest mass of the electron and  $E$  its kinetic energy. Thus, at straight sections of storage rings, moving electrons will produce a narrow and intense mono-directional photon beam. At the synchrotron radiation facilities, where beamlines are channeled out of the storage ring a continuous bremsstrahlung spectrum, with the maximum energy of the particle beam, will be present. This may pose a radiation hazard to the personnel in the experimental floor <sup>1</sup>.

## Experimental Setup and Procedure

Bremsstrahlung energy spectra from insertion device (ID) beamlines at the APS have been measured by a fast and sensitive electromagnetic calorimeter made of 25 lead-glass detectors, each 6.3 cm x 6.3 cm x 35 cm, stacked into a 5x5 array <sup>1,2</sup>. The energy resolution of this detector is  $(7 \pm 2)/\sqrt{E}$  % and the time response is typically 20 ns. The bremsstrahlung beam is aligned along the central lead-glass detector. The central 3 x 3 detector matrix of the calorimeter has been found to contain 100% of the electromagnetic shower in the lateral direction and approximately 96 % in the longitudinal direction. Energies of the incident bremsstrahlung photons are measured on an event-per-event basis. Individual lead-glass detector signals are read through the phototmultiplier tubes; the signals are then fed into fast encoding and readout ADCs (FERA). The signal from the central lead-glass detector is split into a trigger circuit that is used to generate a trigger to ADCs upon real energy deposition. Digitized data from ADCs are stored into a 16K memory unit for subsequent slow readout by a computer. A schematic of the calorimeter and associated data acquisition system is shown in Figure 1. A more detailed description of the experimental set up is given elsewhere <sup>2,3</sup>.

The intensity of gas bremsstrahlung is a function of the stored beam current, atomic number of residual gas, and the storage-ring vacuum. Thus, during the experimental runs, data have been collected in order to determine the correct value of the storage-ring vacuum and the molecular composition of the residual gas inside the storage ring. The variation of average vacuum in the straight section, as determined by six ion gauges, is shown in Figure 2A and 2B for beamlines 11 ID and 6 ID respectively. The vacuum can be seen to vary linearly within the beam current range (50 mA to 100 mA) that was available during the measurement. Table 1 shows typical residual gas component information measured at 11 ID and 6 ID at a given beam current.

## Results and Discussion

The data in this report come from two separate experimental runs: one conducted in October-November 1997 and the other in March 1998. The first run was conducted at beamline 11-ID and the latter at beamline 6-ID. The calibration procedure for the lead-glass calorimeter, the nature of the raw ADC bremsstrahlung distributions, and various systematic corrections involved are discussed elsewhere <sup>2,3</sup>. Figure 3A and 3B show measured bremsstrahlung energy spectra, normalized to storage-ring vacuum, for a few typical beam currents of the two experimental runs. Systematic corrections associated with the measurements such as dead-time losses, longitudinal shower leakage, and low energy cutoff, have been applied to the energy spectra in Figure 3 to obtain the corrected results shown in Tables 2 and 3. Results from Table 2 and Table 3 are also shown plotted in Figure 4A and 4B. Figure 4A shows the variation in bremsstrahlung energy, normalized to the beam current, as a function of the storage-ring vacuum. Figure 4B gives the variation of the bremsstrahlung energy, normalized to both the vacuum and beam current, as a function of beam current. The bremsstrahlung contribution from each individual sector is fairly constant (as seen in Figure 4B)- an average of  $118 \pm 9$  GeV/s/nT/mA from 11-ID and  $36 \pm$  GeV/s/nT/mA from 6-ID. The bremsstrahlung power in kilowatts, normalized to the storage-ring vacuum, is given in Figure 5 for the two beamlines as a function of the beam current. It is clear that the power varies linearly with the beam current. The average normalized bremsstrahlung powers of  $(2.0 \pm 0.2) \times 10^{-8}$  W/nT/mA and  $(0.6 \pm 0.03) \times 10^{-8}$  W/nT/mA have been measured for beamline 11 ID and 6 ID respectively.

## Conclusions

Independent measurements of normalized bremsstrahlung power from six beamlines at the Advanced Photon Source (the present two and four earlier measurements <sup>2,3</sup>) have shown a variation of as much as a factor of ten. Clearly, bremsstrahlung power varies with beam current and storage-ring vacuum. Bremsstrahlung power, normalized to the storage-ring vacuum and the beam current, is fairly constant within a beamline for a given storage ring fill pattern but may vary from beamline to beamline. The reasons for such a beamline-to-beamline variation of the normalized bremsstrahlung power are attributed to the variation of the vacuum profile along the vacuum chamber, variation of the residual gas composition in the straight section, the variation of temperature profile along the vacuum chamber due to RF heating, and the presence of a non-gas bremsstrahlung component. The production of the non-gas bremsstrahlung component depends upon the vacuum chamber dimensions, relative position of the beam with respect to the vacuum chamber, and the maximum bunch current in the storage ring as determined

by the storage-ring fill pattern. The normalized bremsstrahlung power may vary due to any or a combination of the reasons discussed above. This makes comparing the results of various bremsstrahlung measurements difficult.

## References

- [1] Moe, H. J., Advanced Photon Source- Radiological Design Considerations, ANL-APS-LS-141, Argonne National Laboratory, July 1991.
- [2] Pisharody, M., et al., Measurement of Gas Bremsstrahlung from the Insertion Device Beamlines of the Advanced Photon Source, ANL-APS-LS 260 Argonne National Laboratory, March 1997.
- [3] Pisharody, M., et al., Measurement of Gas Bremsstrahlung from Electron Storage Rings, Nucl. Instr. Meth. A 401, 442, 1997.

Table 1: Typical residual gas measurement results for beamlines 11-ID and for 6-ID at a given beam current.

Beamline	Mass Number	Residual Gas Component	Mole Fraction (%)	Weight Percent (%)
11-ID	2	H <sub>2</sub>	80.0	25.9
	16	CH <sub>4</sub>	4.5	11.7
	19	F	5.7	17.7
	28	N <sub>2</sub> /CO	9.8	44.7
6-ID	2	H <sub>2</sub>	57.4	8.3
	18	H <sub>2</sub> O	13.1	17.0
	28	N <sub>2</sub> /CO	16.4	33.1
	44	CO <sub>2</sub>	13.1	41.6

Table 2: Bremsstrahlung power for various beam currents from the 15.38 m of positron beam straight path at beamline 11-ID. A 12% correction due to the threshold cut-off was determined in the photon count rate and has been incorporated in the bremsstrahlung photon rate.

Beam Current $I_b$ (mA)	Estimated Vacuum $P$ (nT)	Bremsstrahlung Photon Rate $N_\gamma$ (/s/nT/mA)	Bremsstrahlung Energy Rate $E_\gamma$ (GeV/s/nT/mA)
63.0	6.33	50±4	99±9
70.1	7.18	55±4	108±9
71.6	7.19	55±4	108±9
72.0	7.35	55±4	108±9
73.4	7.32	61±4	117±9
74.2	7.51	58±4	114±9
76.0	7.53	56±4	109±9
76.1	7.59	60±4	118±9
77.3	7.70	57±4	112±9
78.4	7.77	60±4	116±9
79.4	7.80	61±4	117±9
80.3	7.88	60±4	119±9
80.5	8.09	60±4	116±9
81.1	8.08	61±4	117±9
82.1	8.08	61±4	120±9
82.2	8.13	55±4	111±9
84.0	8.30	64±4	122±9
86.3	8.42	65±4	123±9
88.4	8.67	65±4	125±9
88.9	8.63	68±4	128±9
89.6	8.69	65±4	126±9
91.4	8.91	68±4	129±9
92.2	8.90	65±4	126±9
92.8	8.89	64±4	121±9
94.6	9.10	68±4	129±9
96.0	9.18	70±4	129±9
97.4	9.37	67±4	126±9

Table 3: Bremsstrahlung power for various beam currents from the 15.38 m of positron beam straight path at beamline 6-ID. A 12% correction due to the threshold cut-off was determined in the photon count rate and has been incorporated in the bremsstrahlung photon rate.

Beam Current $I_b$ (mA)	Estimated Vacuum $P$ (nT)	Bremsstrahlung Photon Rate $N_\gamma$ (/s/nT/mA)	Bremsstrahlung Energy Rate $E_\gamma$ (GeV/s/nT/mA)
52.1	5.89	21±1	35±2
54.1	6.18	19±1	33±2
61.2	6.80	21±1	35±2
61.4	6.86	19±1	34±2
64.9	7.18	19±1	34±2
66.8	7.41	21±1	35±2
73.4	7.91	20±1	35±2
73.9	7.89	19±1	34±2
76.3	8.13	21±1	35±2
76.3	8.20	21±1	35±2
79.8	8.50	20±1	35±2
80.2	8.52	21±1	36±2
82.1	8.76	19±1	35±2
83.5	8.90	20±1	36±2
84.8	8.97	22±1	36±2
84.8	8.91	22±1	37±2
86.3	9.04	22±1	37±2
86.8	9.06	22±1	37±2
87.2	9.07	20±1	36±2
88.2	9.28	22±1	36±2
89.5	9.42	22±1	36±2
90.0	9.39	22±1	37±2
90.2	9.34	22±1	37±2
92.0	9.60	23±1	38±2
93.4	9.68	22±1	37±2
93.4	9.62	22±1	37±2
93.6	9.59	20±1	36±2
94.0	9.70	22±1	37±2
96.0	10.01	22±1	37±2
96.2	9.99	21±1	37±2
96.2	9.98	20±1	36±2
99.7	10.21	22±1	37±2
100.6	10.21	19±1	33±2
101.6	10.51	20±1	35±2

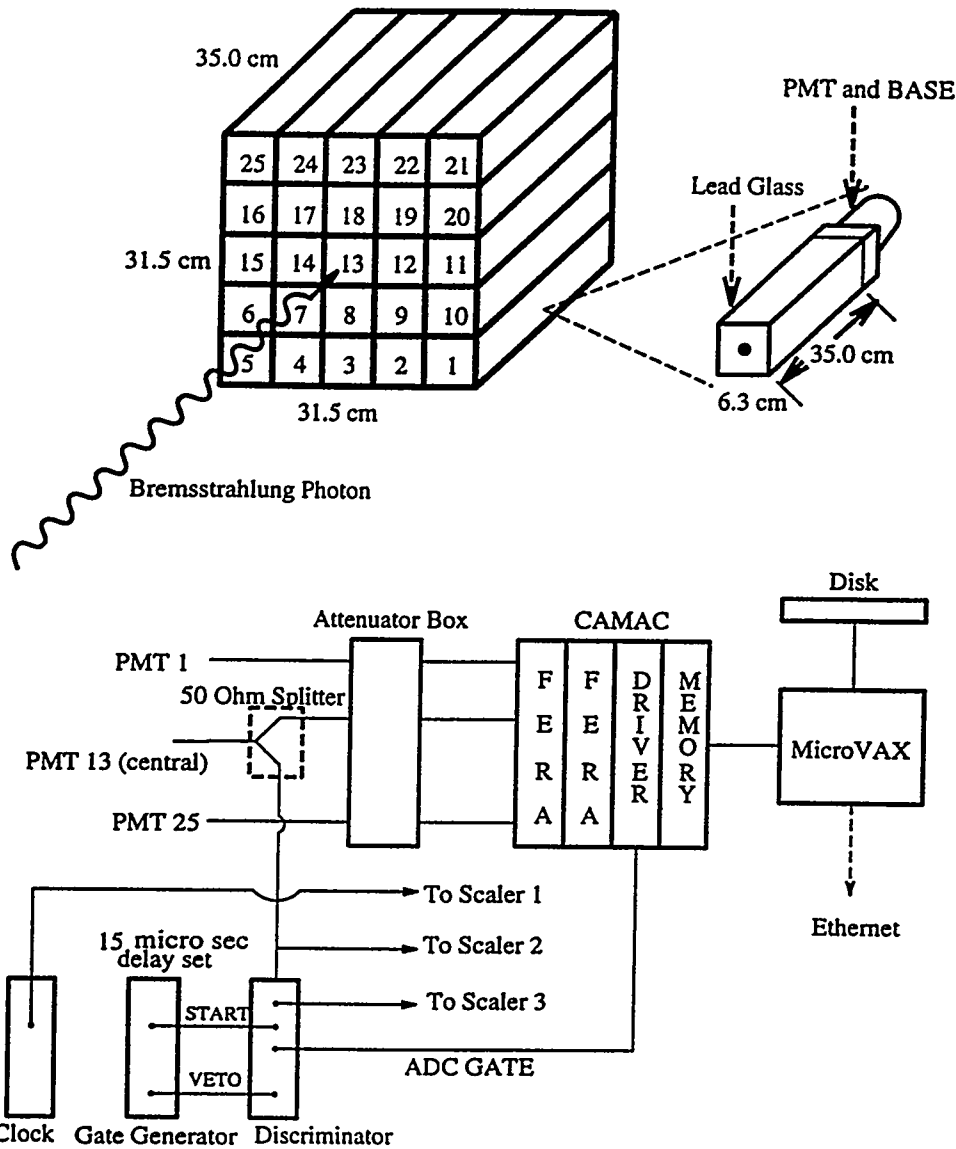


Figure 1: The lead-glass electromagnetic calorimeter and associated data acquisition system that are used to measure the bremsstrahlung spectrum and power.

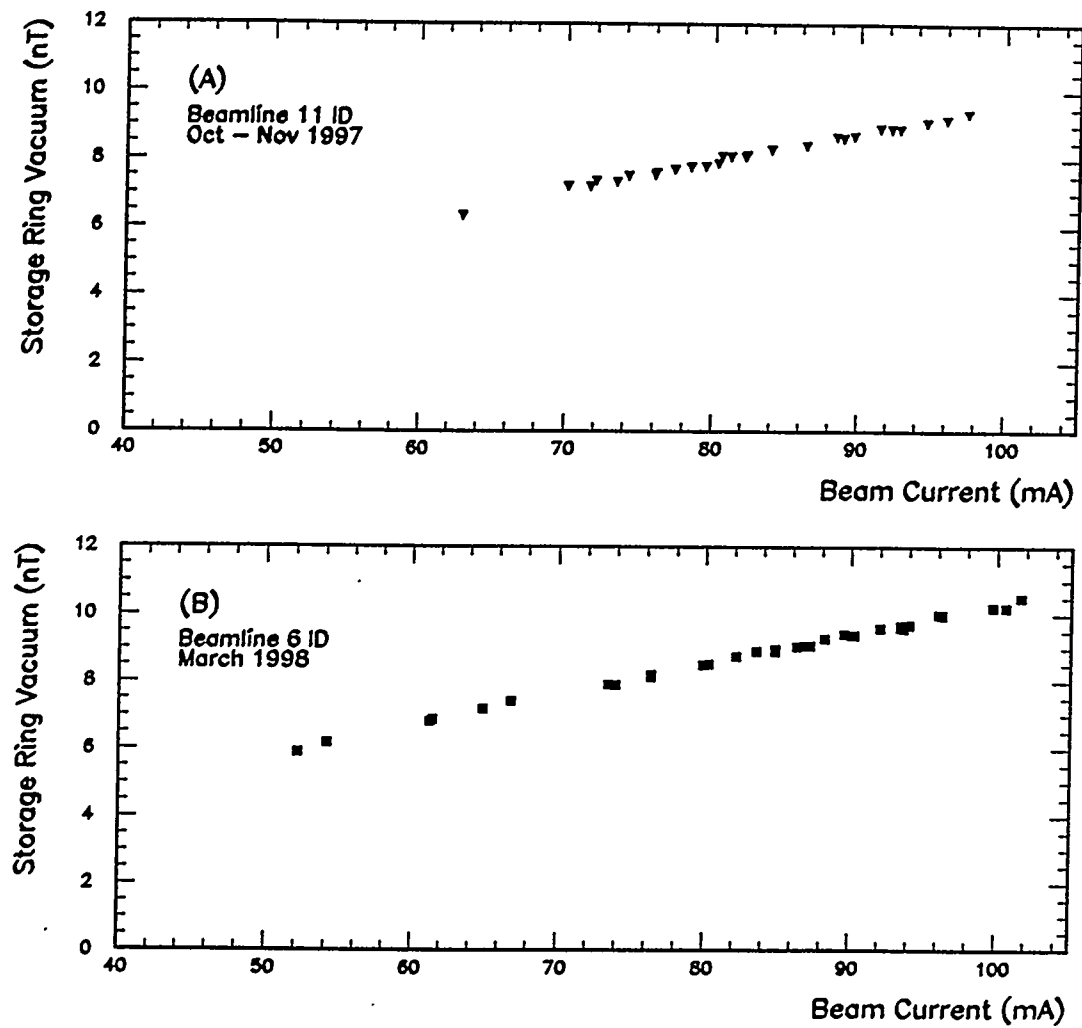


Figure 2: Variation of storage ring vacuum as a function of beam current at beamlines 11-ID and 6-ID.

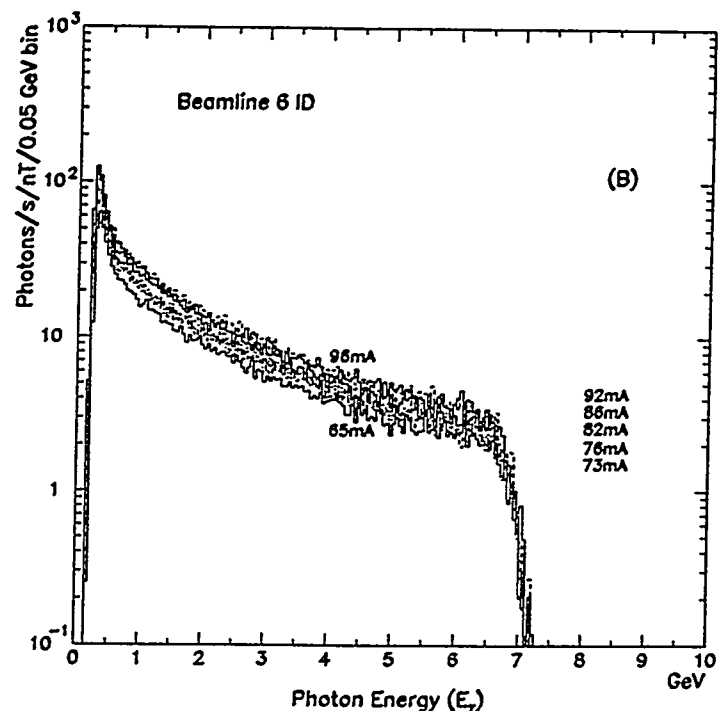
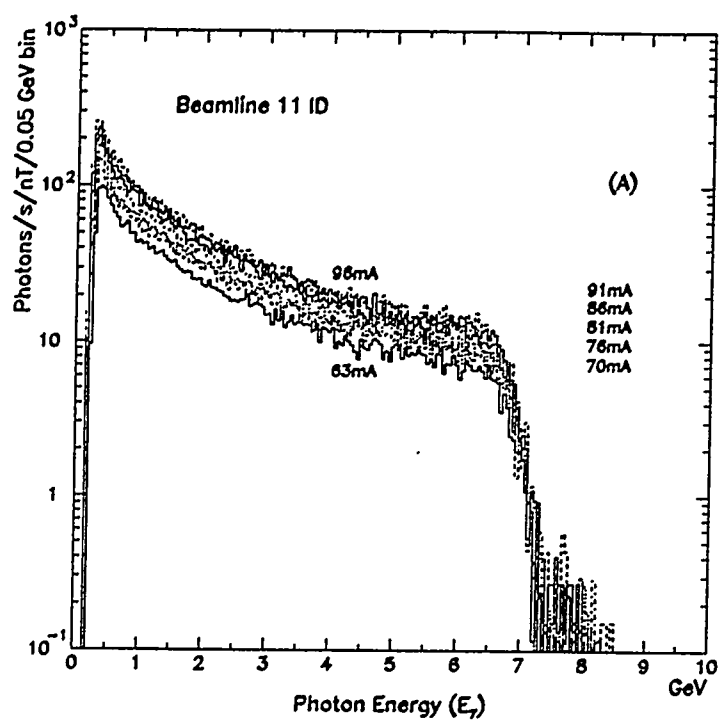


Figure 3: Bremsstrahlung energy spectra, corrected for dead-time losses, for typical beam currents during the two experimental runs at beamlines 11-ID (A) and 6-ID (B).

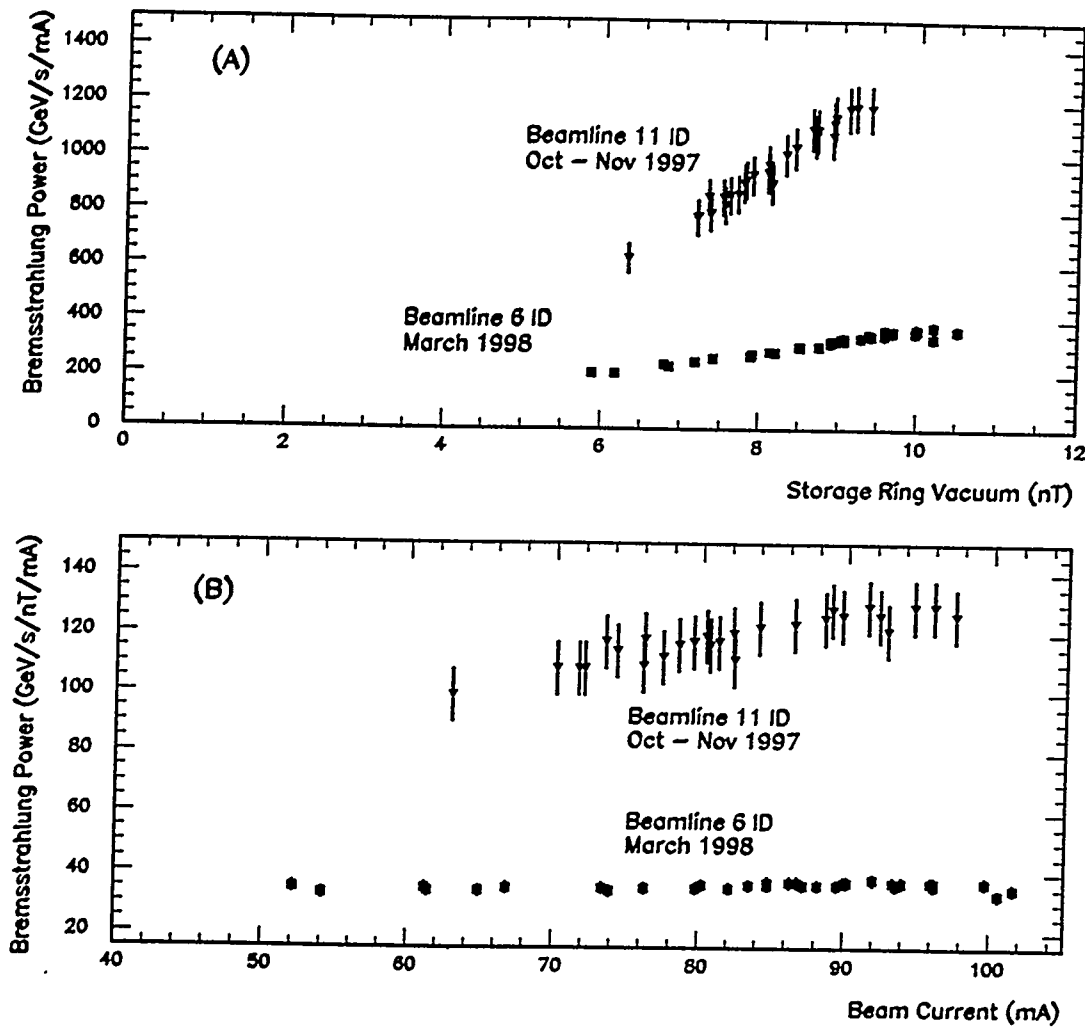


Figure 4: (A) Bremsstrahlung power, normalized to beam current, as a function of the storage ring vacuum for the two experimental runs at beamlines 11-ID and 6-ID. (B) The slopes of the lines in (A), which give the normalized bremsstrahlung contribution from both beamlines, as a function of the beam current.

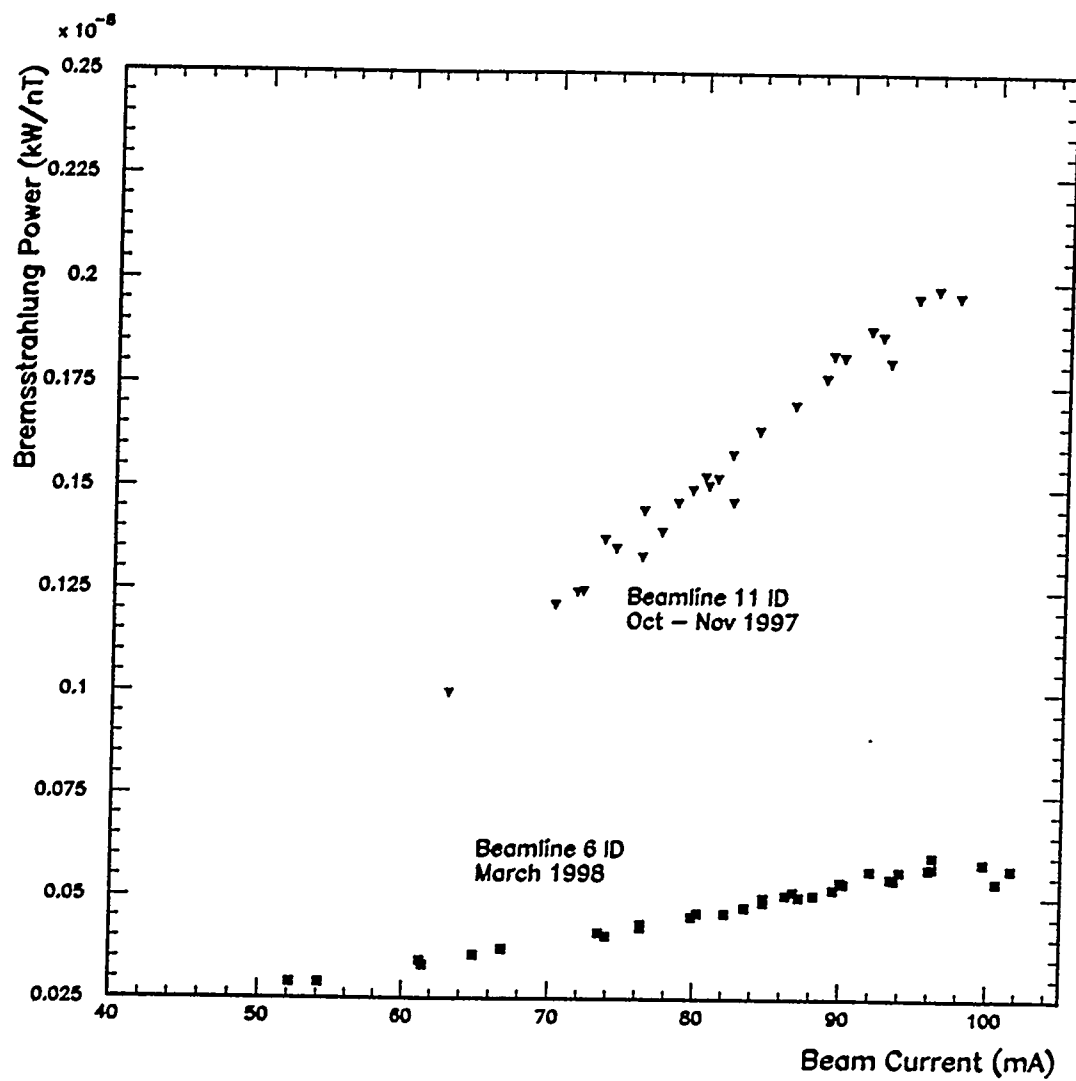


Figure 5: Bremsstrahlung power in kilowatts, normalized to the storage ring vacuum, as a function of the beam current for the two experimental runs at beamlines 11-ID and 6-ID.